Materials Research. 2014; 17(1): 186-189
DOI: http://dx.doi.org/10.1590/S1516-14392013005000171

Giant Reversible Magnetocaloric Effect in Flower-like β-$Co(OH)_2$ Hierarchical Superstructures Self-assembled by Nanosheets

Xianguo Liu[a]*, Chao Feng[a], Feng Xiao[a], Siu Wing Or[b], Yuping Sun[c], Chuangui Jin[a], Ailin Xia[a]

[a]*Anhui Key Laboratory of Metal Materials and Processing, School of Materials Science and Engineering, Anhui University of Technology, Ma'anshan 243002, PR China*
[b]*Department of Electrical Engineering, The Hong Kong Polytechnic University, Hung Hom, Kowloon, Hong Kong*
[c]*Center for Engineering practice and Innovation Education, Anhui University of Technology, Ma'anshan 243002, PR China*

Received: February 15, 2013; Revised: September 4, 2013

A facile hydrothermal strategy is proposed to synthesize flower-like β-$Co(OH)_2$ hierarchical microspherical superstructures with a diameter of 0.5-1.5 µm, which are self-assembled by β-$Co(OH)_2$ nanosheets with the average thickness ranging between 20 and 40 nm. The magnetocaloric effect associated with magnetic phase transitions in $Co(OH)_2$ superstructures has been investigated. A sign change in the magnetocaloric effect is induced by a magnetic field, which is related to a filed-induced transition from the antiferromagnetic to the ferromagnetic state below the Néel temperature. The large reversible magnetic-entropy change $-\Delta S_m$ (13.4 J/kg K at 15 K for a field change of 5 T) indicates that flower-like $Co(OH)_2$ superstructures is a potential candidate for application in magnetic refrigeration in the low-temperature range.

Keywords: *magnetic materials, nanocomposites, nanoparticles*

1. Introduction

Currently, there is a great deal of interest in utilizing the magnetocaloric effect (MCE) as an alternate technology for refrigeration, replacing the common gas-compression expansion technology, due to higher efficiency and environmental concerns[1-11]. An ideal material for magnetic refrigeration should be composed of relatively inexpensive raw materials, have a high MCE demonstrated by a high change in magnetic entropy (ΔS_M) and a high adiabatic temperature change, and have little or no thermal/magnetic hysteresis[1,8]. The giant MCE, closely associated with the first-order magnetic transition (FOMT), has been observed in different systems[1]. Unfortunately, the FOMT usually leads to considerable thermal and magnetic irreversibility which is disadvantageous for application. Therefore, much attention has been recently focused on finding new materials with a large MCE and a small thermal/magnetic hysteresis. A giant MCE has been observed in antiferromagnetic (AFM) systems, originating from a field-induced transition from a collinear AFM to a triangular AFM [(or ferromagnetic (FM)] state[1,11]. Furthermore, as the thermal/ magnetic hysteresis is quite small for AFM systems, compared with giant-MCE ferromagnetic (FM) materials, they may be more suitable for application on the aspect of refrigerant efficiency and energy conservation. In the past decade, there has been a growing interest in the investigation of superstructures self-assembled by nanosheets due to the interesting properties they possess, owing to their high anisotropy and thinness[7,12.] A few investigations have been focused on the preparation and magnetic properties of cobalt hydroxide β-$Co(OH)_2$[1,7]. In this work, we synthesize the flower-like $Co(OH)_2$ hierarchical superstructures self-assembled by nanosheets and study the magnetic and magnetocaloric properties of the superstructures at low temperatures. A giant negative magnetic-entropy change is found together with a field-induced MCE conversion (the MCE changes its sign in the applied magnetic field).

*e-mail: liuxianguohugh@gmail.com; eeswor@polyu.edu.hk

2. Experimental Section

Analytically pure reagents were used in this experiment. A mixture was prepared by mixing water, ethanol and glycol amine in 20:1:10 volume ration, and then 0.2 mmol $Co(NO_3)_2{\cdot}6H_2O$ was dissolved in the 40 mL above mixture under stirring. This solution was stirred for 30 min, after which it was transferred into a 50-mL Telfon-lined stainless tell autoclave. The autoclave was sealed and maintained at 180 °C for 12 h and then cooled to room temperature naturally. The products obtained after hydrothermall treatment were centrifuged, washed with distilled water and ethanol several times and finally dried in vacuum at 60 °C for 4h. The as-prepared sample was characterized by x-ray diffraction (XRD, Bruker D8) and scanning electron microscopy (SEM, JEOL-6300 F) and transmission electron microscopy (TEM, JEOL JEM-2010). The magnetization measurements were carried out using a superconducting quantum interference device (SQUID, Quantum Design MPMS XL-7). The MCE is characterized by the isothermal magnetic-entropy change. By using the Maxwell relation

$(\partial S / \partial B)_T = (\partial M / \partial T)_B$, the magnetic-entropy change can be represented as

$$\Delta S_M(T,B) = S_M(T,B) - S_M(T,0) = \int_0^B \left(\frac{\partial S_M}{\partial B}\right)_T dB = \int_0^B \left(\frac{\partial M}{\partial B}\right)_B dB \qquad (1)$$

3. Results and Discussion

The XRD pattern of the as-synthesized flower-like $Co(OH)_2$ hierarchical supersturcutures is illustrated in Figure 1a. Five obvious diffraction peaks can be easily identified for the (001), (100), (011), (012) and (110) planes of the hexagonal β-$Co(OH)_2$ crystalline structure, respectively. No peaks of any other phases or impurities are detected, suggesting high purity of the as-prepared pink $Co(OH)_2$ sample. Figure 1b, c demonstrate the SEM images of the $Co(OH)_2$ samples with different magnifications. The as-synthesized $Co(OH)_2$ sample presents a uniform flower-like microspheres with a diameter of 0.5-1.5µm , as seen from Figure 1b. Furthermore, the magnified SEM images (Figure 1c) demonstrate that three-dimensional flower-like microspheres are self-assembled by lots of $Co(OH)_2$ nanosheets building blocks with the average thickness ranging between 20 and 40 nm. It is worthwhile noting that the as-obtained flower-like $Co(OH)_2$ superstructures cannot be destroyed and broken into the individual $Co(OH)_2$ nanosheets even after subjecting long-time ultrasonication. In addition, the TEM image in Figure 1d clearly shows that the d-spacing of 0.236 nm corresponds to the lattice plane {011} of β-$Co(OH)_2$.

The temperature dependences of the magnetic susceptibility and the inverse magnetic susceptibility in a magnetic field of 0.01 T are shown in Figure 2a. A sign of AFM transition at Néel temperature $T_N \approx$ 10 K can be found from the 1/χ-T curve, which is lower than the previously reported values of 11 and 12.3 K in References[1,8], respectively. A decrease in T_N is observed in many nanosized AFM systems as the grain size decreased[1,7]. The magnetic hysteresis loop at 5 K in an applied field of 5 T is shown in Figure 2b. It can be noticed that the coercivity of 0.014 T is extremely small and the remanent magnetization is close to zero. Furthermore, there is nearly zero magnetic hysteresis in the transition field. $Gd_5(Ge_{1-x}Si_x)_4$ as a typical giant-MCE material has the magnetic hysteresis of about 1 T near the magnetic-transition temperature[10]. The small magnetic hysteresis of β-$Co(OH)_2$ is advantageous for application. In addition, it should be noted that the M-H loop shows step-type line (field-induced AFM to FM behavior) at 5 K[7].

Figure 2c shows the isothermal magnetization curves of the β-$Co(OH)_2$ superstructures , which are plotted as

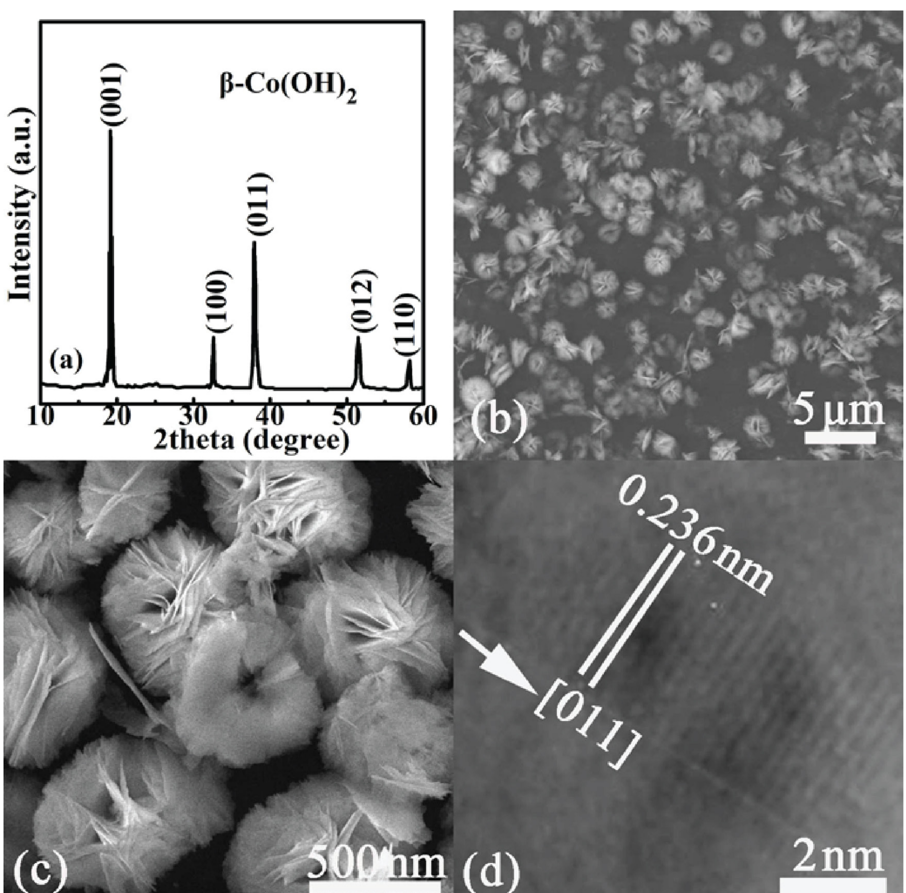

Figure 1. (a) XRD pattern, (b) and (c) SEM images with different magnifications for the flower-like $Co(OH)_2$ superstructures, and (d) TEM image of $Co(OH)_2$ nanosheets.

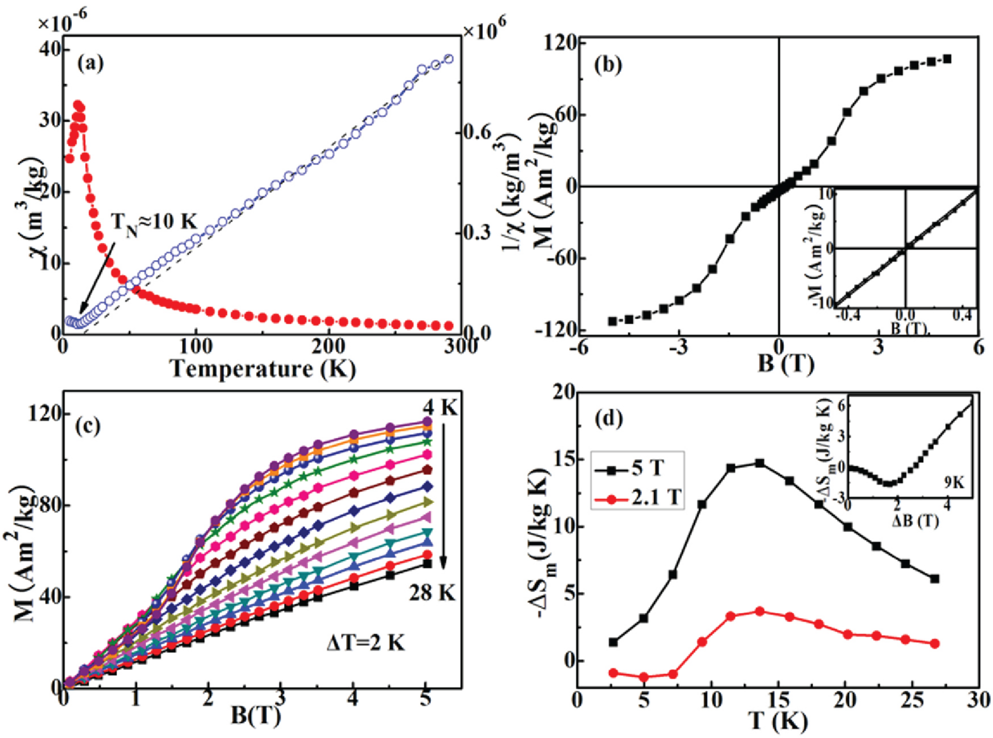

Figure 2. (a) Temperature dependence of the magnetic susceptibility and the inverse magnetic susceptibility of $Co(OH)_2$ measured at an applied magnetic field of 0.01 T. (b) Magnetic hysteresis loop of at 5 K in applied fields up to 5 T. Inset: the hysteresis loop at 5 K in low fields. (c) Magnetic isotherms of $Co(OH)_2$ measured between 4 and 28 K with a temperature step of 2 K. (d) Negative magnetic-entropy change $-\Delta S_m$ verse temperature T curves for different magnetic field changes (ΔB). Inset: $-\Delta S_m$ as a function of ΔB at 9 K.

a function of the applied magnetic field (ranging from B = 0 to 5 T) between 4 and 28 K with ΔT = 2 K. Below T_N, the magnetization increases gradually with the applied field in the low-field range and then jumps at a critical field but remains unsaturated at 5 T. The step in the magnetization curves indicates a clear field-induced AFM to FM phase transition[1].

A large MCE is expected around T_N where the magnetization rapidly changes with varying temperature. The isothermal entropy change is derived from the magnetization data in Figure 2c according to Equation 1. The curves of $-\Delta S_m$ versus T are given in Figure 2d. It can be seen that, for small magnetic-field changes, $-\Delta S_m$ is negative below T_N, whereas it changes to small positive values with increasing temperature[1]. Usually, the inverse MCE is observed in first-order magnetic transitions such as AFM/FI, AFM/FM, or collinear AFM/triangular AFM[1,11]. The inverse MCE has also been reported in AFM/PM transition systems, in which the applied field results in a further spin-disordered state near the transition temperature, which increases the configurational entropy[1,13,14]. The inset in Figure 2d presents $-\Delta S_m$ versus ΔB at 9 K, where a minimum value of –1.62 J/kg K of $-\Delta S_m$ is found for ΔB=1.7 T. The applied field destroys the antiparallel alignment of the spin moments, and the spin disorder will result in a negative $-\Delta S_m$, becoming more negative with increasing applied field. However, the value of $-\Delta S_m$ increases with further increasing magnetic field due to the field-induced transition from the AFM to the FM state and becomes positive at 2.7 T. The field-induced AFM to FM transition is responsible for the conversion from the inverse to the conventional MCE in β-$Co(OH)_2$. The maximum of $-\Delta\Sigma_m$ of 13.4 J/kg K at K for ΔB = 5T, which is comparable with giant MCE reported for La-Fe-Si, MnAs and Mn-Fe-P based alloy[15]. The slope of the curve in Figure 2d is relatively small, and the smooth variation in $-\Delta S_m$ with temperature is more useful than a sharp one, which is another property that makes it a promising magnetic refrigerant.

4. Conclusions

In summary, we propose an efficient synthetic strategy to synthesize the flower-like $Co(OH)_2$ hierarchical superstructures, which are self-assembled by $Co(OH)_2$ nanosheets. This material displays a large magnetic entropy change of 13.4 J/kg K almost without hysteresis at 15 K in a magnetic field change of 5 T, thereby indicating the suitability of this material for use in magnetic refrigeration.

Acknowledgements

This study has been supported partly by the National Natural Science Foundation of China (Grant Nos. 51201002, 11204003 and 21071003), by the Research Grants Council of the HKSAR Government (PolyU 5236/12E), and by The Hong Kong Polytechnic University (G-YK59 and 4-ZZ7L).

References

1. Liu XH, Liu W, Hu WJ, Guo S, Lv XK and Cui WB. Giant reversible magnetocaloric effect in cobalt hydroxide nanoparticles. *Applied Physics Letters.* 2008; 93(20):202502. http://dx.doi.org/10.1063/1.3028337
2. Liu XG, Geng DY, Du J, Ma S, Li B, Shang PJ et al. The large cryogenic magnetocaloric effect of $TbAl_2$ nanocapsules. *Scripta Materilia.* 2008; 59(3):340-343. http://dx.doi.org/10.1016/j.scriptamat.2008.04.005
3. Liu XG, Geng DY, Zhang Q, Jiang JJ, Liu W and Zhang ZD. Microstructure and magnetic properties of graphite-coated Gd nanocapsules. *Applied Physics Letters.* 2009; 94(10):103104. http://dx.doi.org/10.1063/1.3100618
4. Liu XG, Or SW, Li B, Ou ZQ, Zhang L, Zhang Q et al. Magnetic properties of Dy nanoparticles and Al_2O_3-coated Dy nanocapsules. *Journal of Nanoparticle Research.* 2011; 13(3):1163-1174. http://dx.doi.org/10.1007/s11051-010-0108-y
5. Liu XG, Geng DY, Jiang JJ, Li B, Ma S, Li D et al. Magnetic properties and large cryogenic low-filed magnetocaloric effect of $HoCo_2$ nanoparticles without core/shell structure. *Journal of Nanoparticle Research.* 2010; 12(4): 1167-1172. http://dx.doi.org/10.1007/s11051-009-9717-8
6. Liu XG, Li B, Geng DY, Shi CX, Yang F, Kang DJ et al. Formation and large cryogenic magnetocaloric effect of $HoAl_2/Al_2O_3$ nanocapsules. *Journal of Physics D:* Applied Physics. 2009; 42(4):045008. http://dx.doi.org/10.1088/0022-3727/42/4/045008
7. Shamba P, Zeng R, Wang JQ and Dou SX. A sign of field-induced first order magnetic state transition and giant reversible magnetocaloric effect in cobalt hydroxide nanosheets. *Journal of Applied Physics*. 2010; 107(9):09A919.
8. Takada T, Bando Y, Kiyama M and Miyamoto H. The magnetic property of β-$Co(OH)_2$. *Journal of Physical Society of Japan.* 1966; 21(2):2726-2727. http://dx.doi.org/10.1143/JPSJ.21.2726
9. Samanta T, Das I and Banerjee S. Giant magnetocaloric effect in antiferromagnetic $ErRu_2S_{i2}$ compound. *Applied Physics Letters.* 2007; 91(15):152506. http://dx.doi.org/10.1063/1.2798594
10. Pecharsky VK and Gschneidner KA Jr. Giant magetocaloric effect in $Gd_5(Si_2Ge_2)$. *Physial Review Letters.* 1997; 78(23):4494-4497. http://dx.doi.org/10.1103/PhysRevLett.78.4494
11. Du J, Cui WB, Zhang Q, Ma S, Xiong DK and Zhang ZD. Giant magnetocaloric effect in ε-$(Mn_{0.83}Fe_{0.17})_{3.25}Ge$ antiferromagnet. *Applied Physics Letters.* 2007; 90(4):042510. http://dx.doi.org/10.1063/1.2432274
12. Hu JQ, Bando Y, Zhan JH, Li YB and Sekiguchi T. Two-diemnsional micrometer-sized single-crystalline ZnO thin nanosheets. *Applied Physics Letters.* 2003; 83(21):4414-4416. http://dx.doi.org/10.1063/1.1629788
13. Hu WJ, Du J, Li B, Zhang Q and Zhang ZD. Giant anomalous magnetocaloric effect in DySb Ising antiferromagnet. *Applied Physics Letters.* 2008; 92(19):192505. http://dx.doi.org/10.1063/1.2928233
14. Krenke T, Duman E, Acet M and Wassermann EF. Inverse magnetocaloric effect in ferromagnetic Ni-Mn-Sn alloys. *Nature Materials.* 2005; 4: 450-454. http://dx.doi.org/10.1038/nmat1395
15. Sandeman KG. Magnetocaloric materials: The search for new systems. *Scripta Materialia.* 2012; 67(6):566-571. http://dx.doi.org/10.1016/j.scriptamat.2012.02.045